



# CHORUS

This is the accepted manuscript made available via CHORUS. The article has been published as:

## Comparison of the electromagnetic responses of $^{12}\text{C}$ obtained from the Green's function Monte Carlo and spectral function approaches

Noemi Rocco, Alessandro Lovato, and Omar Benhar

Phys. Rev. C **94**, 065501 — Published 23 December 2016

DOI: [10.1103/PhysRevC.94.065501](https://doi.org/10.1103/PhysRevC.94.065501)

# Comparison of the electromagnetic responses of $^{12}\text{C}$ obtained from the Green's function Monte Carlo and spectral function approaches

Noemi Rocco,<sup>1,2</sup> Alessandro Lovato,<sup>3</sup> and Omar Benhar<sup>1</sup>

<sup>1</sup>*INFN and Department of Physics, "Sapienza" University, I-00185 Roma, Italy*

<sup>2</sup>*Instituto de Fisica Corpuscular (IFIC), Centro Mixto CSIC-Universidad de Valencia, Institutos de Investigacion de Paterna, E-46071 Valencia, Spain*

<sup>3</sup>*Physics Division, Argonne National Laboratory, Argonne, Illinois 60439, USA*

The electromagnetic responses of carbon obtained from the Green's function Monte Carlo and spectral function approaches using the same dynamical input are compared in the kinematical region corresponding to momentum transfer in the range 300–570 MeV. The results of our analysis, aimed at pinning down the limits of applicability of the approximations involved in the two schemes, indicate that the factorization *ansatz* underlying the spectral function formalism provides remarkably accurate results down to momentum transfer as low as 300 MeV. On the other hand, it appears that at 570 MeV relativistic corrections to the electromagnetic current not included in the Monte Carlo calculations may play a significant role in the transverse channel.

PACS numbers: 24.10.Cn, 25.30.Fj, 25.30.Pt

## I. INTRODUCTION

Understanding neutrino-interactions with nuclei in the broad kinematical region relevant to long-baseline neutrino-oscillation experiments is a challenging many-body problem, whose solution requires an accurate and consistent description of the nuclear initial and final states, as well as of the interaction vertex. These elements are in fact intimately connected, as the Hamiltonian determining the nuclear wave functions is related to the currents entering the definition of the transition operators through the continuity equation. In addition, for large values of the momentum transfer, a full account of relativistic effects and the resonance production mechanism is required.

The payoff of this endeavor is high, as it will lead to a significant reduction of the systematic uncertainties associated with the determination of oscillation parameters. In addition, a comparison between theoretical predictions and experimental data will provide a great deal of previously unavailable information, allowing to test the existing models of nuclear interactions and currents, notably in kinematical regions sensitive to the high-momentum components of the nuclear wave function. As an example, signatures of nuclear short-range correlations arising from the non-central component of the nucleon-nucleon (NN) force have been recently identified in charge-changing neutrino-nucleus interactions observed in the Liquid Argon Time Projection Chamber of the ArgoNeuT Collaboration [1, 2].

Electroweak currents are usually tested on transitions of light nuclei, characterized by extremely low momentum transfer. Validating these currents in neutrino-nucleus scattering calculations would corroborate their applicability in the lower energy window, down to 20–30 MeV, which is of great relevance for the physics of supernovae. Finally, probing the high-momentum region is potentially relevant for the ongoing and planned

searches of neutrinoless double-beta ( $0\nu\beta\beta$ ) decay. In fact, unlike the standard  $2\nu\beta\beta$  process, in the  $0\nu\beta\beta$  decay the virtuality of the neutrino in the intermediate state makes the nuclear matrix element sensitive to the high momentum components of the nuclear wave function.

The measurement of a Charged Current Quasi Elastic (CCQE) cross section largely exceeding the predictions of the Relativistic Fermi Gas Model (RFGM), reported by the MiniBooNE collaboration [3, 4], has clearly exposed the need for a more accurate model of neutrino-nucleus interactions, whose development will require a cross-disciplinary transfer of knowledge between nuclear theorists, neutrino experimentalists and the developers of simulation codes. In the pioneering works of Martini *et al.* [5, 6] and Nieves *et al.* [7, 8], the discrepancy between theory and data has been ascribed to reaction mechanisms other than single nucleon knock out, such as those involving meson-exchange currents (MEC), leading to the occurrence of many-particle many-holes final states. The contributions of MEC, evaluated within the RFGM, have been also included in the phenomenological approach based on the scaling analysis of electron-nucleus scattering data [9–11]. While being remarkably successful in explaining MiniBooNE data, however, these models are all based on a somewhat oversimplified description of the underlying nuclear dynamics.

Over the past decade, *ab initio* approaches have reached the degree of maturity needed to describe lepton-nucleus scattering processes starting from a realistic model of the interactions among the nucleons and between them and the beam particle. For instance, the electric dipole response of  $^{16}\text{O}$  and  $^{40}\text{Ca}$  has been computed combining the Lorentz integral transform with the coupled-cluster many-body technique [12, 13]. The Green's Function Monte Carlo (GFMC) algorithm has been implemented to perform accurate calculations of the electromagnetic response functions of  $^4\text{He}$  and  $^{12}\text{C}$  in the regime of moderate momentum transfer, which fully include nuclear correlations generated by a state-of-the-

art Hamiltonian and consistent meson-exchange currents [14, 15]. The main drawbacks of this method are its computational cost— $\sim 5$  million core-hours to compute the response functions for a single value of the momentum transfer—and the severe difficulties involved in its extension to include relativistic kinematic and resonance production.

At large momentum transfer, the formalism based on spectral function (SF) and factorization of the nuclear transition matrix elements [16] allows the combination of a fully relativistic description of the electromagnetic interaction with an accurate treatment of nuclear dynamics. Recently, this approach has been generalized to include the contributions of meson-exchange currents leading to final states with two nucleons in the continuum [17, 18]. However, final state interactions (FSI) involving the struck particles are treated as corrections, whose inclusion requires further approximations [19, 20]

In view of the the above considerations, a comparison of the results obtained using different approaches appears to be much needed. Ab initio methods, while not being best suited to study the kinematical region relevant to neutrino experiments, can in fact provide strict benchmarks, valuable to constrain more approximate models in the limit of low momentum transfer.

This article can be seen as a first step in this direction. We report the results of an analysis of the electromagnetic responses of  $^{12}\text{C}$ , obtained from the GFMC and SF approaches in a variety of kinematical setups. Our work is aimed at gauging the accuracy of the factorization approximation and the importance of relativistic effects, in both the kinematics and the current operator. In order to pin down the role played by the elements of the calculations, we only consider one-body terms in the nuclear current, leaving the discussion of two-body MEC to a forthcoming study. It is very important to realize that our comparison is fully legitimate and meaningful, because the SF and GFMC approaches are based on the same dynamical model, in which nuclear interactions are described by a realistic phenomenological Hamiltonian.

In Section II, we outline the derivation of the electromagnetic responses from the electron-nucleus cross section, and discuss the main elements of their description within the GFMC and SF approaches. In Section III we report the results of our analysis, carried out in the kinematical region corresponding to momentum transfer in the range 300–570 MeV, while in Section IV we summarize our findings and state the conclusions.

## II. NUCLEAR RESPONSE

The double differential cross section of the inclusive electron-nucleus scattering process in which an electron of initial four-momentum  $k_e = (E_e, \mathbf{k}_e)$  scatters off a nuclear target to a state of four-momentum  $k_{e'} = (E_{e'}, \mathbf{k}_{e'})$ , the hadronic final state being undetected, can be written

in the one-photon-exchange approximation as

$$\frac{d^2\sigma}{dE_{e'}d\Omega_{e'}} = \frac{\alpha^2}{q^4} \frac{E_{e'}}{E_e} L_{\mu\nu} W_A^{\mu\nu}. \quad (1)$$

In the above equation  $\alpha = 1/137$  is the fine structure constant,  $d\Omega_{e'}$  is the differential solid angle in the direction specified by the vector  $\mathbf{k}_{e'}$ , and  $q = k_e - k_{e'} = (\omega, \mathbf{q})$  is the four momentum transfer. The lepton tensor  $L_{\mu\nu}$  is fully specified by the measured electron kinematical variables. The nuclear response is described by the tensor  $W_A^{\mu\nu}$ , defined as

$$W_A^{\mu\nu}(\mathbf{q}, \omega) = \sum_N \langle 0 | J_A^\mu(q) | N \rangle \langle N | J_A^\nu(q) | 0 \rangle \times \delta^{(4)}(P_0 + q - P_N), \quad (2)$$

where  $|0\rangle$  and  $|N\rangle$  denote the initial and final hadronic states, the four-momenta of which are  $P_0 \equiv (E_0, \mathbf{p}_0)$  and  $P_N \equiv (E_N, \mathbf{p}_N)$ .

The target ground state  $|0\rangle$  does not depend on momentum transfer, and can be safely described using non-relativistic nuclear many-body theory (NMBT). Within this scheme, the nucleus is viewed as a collection of  $A$  pointlike protons and neutrons, whose dynamics are described by the Hamiltonian

$$H = \sum_i \frac{\mathbf{p}_i^2}{2m} + \sum_{j>i} v_{ij} + \sum_{k>j>i} V_{ijk}. \quad (3)$$

In the above equation,  $\mathbf{p}_i$  is the momentum of the  $i$ -th nucleon, while the potentials  $v_{ij}$  and  $V_{ijk}$  describe two- and three-nucleon interactions, respectively. Phenomenological two-body potentials are obtained from an accurate fit to the available data on the two-nucleon system, in both bound and scattering states, and reduce to the Yukawa one-pion-exchange potential at large distances. In this work, we adopt the state-of-the-art Argonne  $v_{18}$  potential [21]. The inclusion of the additional three-body term,  $V_{ijk}$ , is needed to explain the binding energies of the three-nucleon systems and nuclear matter saturation properties [22].

The nuclear electromagnetic current is usually written as a sum of one- and two-nucleon contributions according to

$$J_A^\mu = \sum_i j_i^\mu + \sum_{j>i} j_{ij}^\mu, \quad (4)$$

where the second term in the right hand side—accounting for processes in which the photon couples to a meson exchanged between two interacting nucleons or to the excitation of a resonance (see, e.g., Ref. [23])—is needed for the continuity equation to be satisfied.

In this paper we will discuss the results obtained retaining only the current  $j_i^\mu$ , which describes interactions involving a single nucleon. In the quasi elastic (QE) sector, it can be expressed in terms of the measured proton and neutron vector form factors [24, 25].

Both the current operator and the final nuclear state  $|N\rangle$ , which includes at least one particle carrying a momentum of order  $|\mathbf{q}|$ , explicitly depend on  $\mathbf{q}$ . As a consequence, in the absence of a comprehensive relativistic description of nuclear structure and dynamics, a consistent theoretical calculation of the response tensor is only possible in the kinematical regime corresponding to  $|\mathbf{q}|/m \ll 1$ , with  $m$  being the nucleon mass, where the non relativistic approximation is applicable.

By performing the Lorentz contraction, the double differential cross section of Eq.(1), can be written in terms of the nuclear responses describing interactions with longitudinally (L) and transversely (T) polarised photons

$$\frac{d^2\sigma}{dE'_e d\Omega_e} = \left( \frac{d\sigma}{d\Omega_e} \right)_M \left[ A_L(|\mathbf{q}|, \omega, \theta_e) R_L(|\mathbf{q}|, \omega) + A_T(|\mathbf{q}|, \omega, \theta_e) R_T(|\mathbf{q}|, \omega) \right], \quad (5)$$

where

$$A_L = \left( \frac{q^2}{\mathbf{q}^2} \right)^2, \quad A_T = -\frac{1}{2} \frac{q^2}{\mathbf{q}^2} + \tan^2 \frac{\theta_e}{2}. \quad (6)$$

and  $(d\sigma/d\Omega_e)_M = [\alpha \cos(\theta_e/2)/4E_e \sin^2(\theta_e/2)]^2$  is the Mott cross section.

The  $L$  and  $T$  response functions can be readily expressed in terms of the components of the hadron tensor, *i.e.* of the nuclear current matrix elements of Eq. (4), as

$$R_L = W_A^{00} = \sum_N \langle 0 | J_A^0 | N \rangle \langle N | J_A^0 | 0 \rangle \delta^{(4)}(P_0 + q - P_N), \quad (7)$$

$$R_T = \sum_{ij=1}^3 \left( \delta_{ij} - \frac{q_i q_j}{\mathbf{q}^2} \right) W_A^{ij} = \sum_N \langle 0 | J_A^T | N \rangle \langle N | J_A^T | 0 \rangle \delta^{(4)}(P_0 + q - P_N). \quad (8)$$

Choosing the  $z$ -axis along the direction of the momentum transfer, one finds

$$R_T = W_A^{xx} + W_A^{yy} = \left[ \langle 0 | J_A^x | N \rangle \langle N | J_A^x | 0 \rangle + \langle 0 | J_A^y | N \rangle \langle N | J_A^y | 0 \rangle \right] \delta^{(4)}(P_0 + q - P_N). \quad (9)$$

### A. Quantum Monte Carlo

GFMC is a suitable framework to carry out accurate calculations of a variety of nuclear properties in the non relativistic regime (for a recent review of Quantum Monte Carlo methods for nuclear physics see Ref. [26]).

Valuable information on the L and T responses can be obtained from their Laplace transforms, also referred to as Euclidean responses [27, 28], defined as

$$\tilde{E}_{T,L}(\mathbf{q}, \tau) = \int_{\omega_{el}}^{\infty} d\omega e^{-\omega\tau} R_{T,L}(\mathbf{q}, \omega). \quad (10)$$

The lower integration limit  $\omega_{el} = \mathbf{q}^2/2M_A$ ,  $M_A$  being the mass of the target nucleus, is the threshold of elastic scattering—corresponding to the  $|N\rangle = |0\rangle$  term in the sum of Eq. (2)—the contribution of which is excluded.

Within GFMC, the Euclidean responses are evaluated from

$$\tilde{E}_L(\mathbf{q}, \tau) = \langle 0 | \rho^*(\mathbf{q}) e^{-(H-E_0)\tau} \rho(\mathbf{q}) | 0 \rangle - |\langle 0 | \rho(\mathbf{q}) | 0 \rangle|^2 e^{-\omega_{el}\tau}, \quad (11)$$

and

$$\tilde{E}_T(\mathbf{q}, \tau) = \langle 0 | \mathbf{j}_T^\dagger(\mathbf{q}) e^{-(H-E_0)\tau} \mathbf{j}_T(\mathbf{q}) | 0 \rangle - |\langle 0 | \mathbf{j}_T(\mathbf{q}) | 0 \rangle|^2 e^{-\omega_{el}\tau}, \quad (12)$$

where  $\rho(\mathbf{q})$  and  $\mathbf{j}_T(\mathbf{q})$  denote non relativistic reductions of the nuclear charge and transverse current operators, respectively [29]. Keeping only the leading relativistic corrections, they can be written as

$$\rho_i(\mathbf{q}) = \left[ \frac{\epsilon_i}{\sqrt{1 + Q^2/(4m^2)}} - i \frac{(2\mu_i - \epsilon_i)}{4m^2} \mathbf{q} \cdot (\boldsymbol{\sigma}_i \times \mathbf{p}_i) \right], \quad (13)$$

$$\mathbf{j}_i^T(\mathbf{q}) = \left[ \frac{\epsilon_i}{m} \mathbf{p}_i^T - i \frac{\mu_i}{2m} \mathbf{q} \times \boldsymbol{\sigma} \right], \quad (14)$$

with

$$\epsilon_i = G_E^p(Q^2) \frac{1}{2} (1 + \tau_{z,i}) + G_E^n(Q^2) \frac{1}{2} (1 - \tau_{z,i}),$$

$$\mu_i = G_M^p(Q^2) \frac{1}{2} (1 + \tau_{z,i}) + G_M^n(Q^2) \frac{1}{2} (1 - \tau_{z,i}), \quad (15)$$

where  $G_E^{p(n)}(Q^2)$  and  $G_M^{p(n)}(Q^2)$  are the proton (neutron) electric and magnetic form factors, while  $\boldsymbol{\sigma}_i$  and  $\tau_{z,i}$  are the Pauli matrices describing the nucleon spin and the third component of the isospin, respectively.

Although the states  $|N\rangle \neq |0\rangle$  do not appear explicitly in Eqs. (11) and (12), the Euclidean responses include the effects of FSI of the particles involved in the electromagnetic interaction, both among themselves and with the spectator nucleons.

Inverting the Laplace transform to obtain the longitudinal and transverse response functions from their Euclidean counterparts involves non trivial difficulties. However, maximum-entropy techniques, based on bayesian inference arguments [30, 31], have been successfully exploited to perform accurate inversions, supplemented by reliable estimates of the theoretical uncertainty [14]. In the case of carbon, particular care has to be devoted to the subtraction of contributions arising from elastic scattering and the transitions to the low-lying  $2^+$  and  $4^+$  states [15].

### B. Spectral function formalism

In the kinematical region corresponding to  $\lambda \sim \pi/|\mathbf{q}| \ll d$ ,  $d$  being the average NN distance

in the target nucleus, nuclear scattering can be approximated with the incoherent sum of scattering processes involving individual nucleons. This is the conceptual basis of the Impulse Approximation (IA), which obviously entails neglecting the contribution of the two-nucleon current. Under the further assumption that the struck nucleon is decoupled from the spectator particles, the final state  $|N\rangle$  can be written in a factorized form according to

$$|N\rangle \longrightarrow |\mathbf{p}'\rangle \otimes |R, \mathbf{p}_R\rangle, \quad (16)$$

where  $|\mathbf{p}'\rangle$  is the hadronic state produced at the electromagnetic vertex, with momentum  $\mathbf{p}'$ , and  $|R, \mathbf{p}_R\rangle$  describes the residual system, carrying momentum  $\mathbf{p}_R$ .

Within the IA, the intrinsic properties of both the target nucleus and the spectator system, which are obviously independent of momentum transfer, are described in terms of the spectral function, defined as

$$P(\mathbf{p}, E) = \sum_R |\langle R, \mathbf{p}_R | a_{\mathbf{p}} | 0 \rangle|^2 \delta(E + E_0 - E_R), \quad (17)$$

which can be obtained from NMBT. In the above equation, the operator  $a_{\mathbf{p}}$  removes a nucleon of momentum  $\mathbf{p}$  from the nuclear ground state, leaving the spectator system with an excitation energy  $E$ .

In the QE sector, the nuclear tensor of Eq. (2) can be written as an integral involving the nuclear SF and the incoherent sum of the elementary matrix elements of the one-body current between free nucleon states. The resulting expression is

$$W_A^{\mu\nu} = \int d^3p dE P(\mathbf{p}, E) \sum_i \langle \mathbf{p} | j_i^\mu | \mathbf{p} + \mathbf{q} \rangle \langle \mathbf{p} + \mathbf{q} | j_i^\nu | \mathbf{p} \rangle \\ \times \frac{m^2}{E(\mathbf{p})\mathbf{E}(|\mathbf{p} + \mathbf{q}|)} \delta[\tilde{\omega} + E(\mathbf{p}) - E(|\mathbf{p} + \mathbf{q}|)], \quad (18)$$

with

$$\tilde{\omega} = \omega + m - E - E(\mathbf{p}) = \omega + M_A - E_R - E(\mathbf{p}). \quad (19)$$

The factors  $m^2/(E(\mathbf{p})\mathbf{E}(|\mathbf{p} + \mathbf{q}|))$  have been included to take into account the implicit covariant normalization of quadrispinors of the initial and final nucleons in the matrix element of  $j_i^\mu$ . The right hand side of Eq.(18) can be further rewritten in terms of the quantity

$$w_i^{\mu\nu} = \langle \mathbf{p} | j_i^\mu | \mathbf{p} + \mathbf{q} \rangle \langle \mathbf{p} + \mathbf{q} | j_i^\nu | \mathbf{p} \rangle \\ \times \delta[\tilde{\omega} + E(\mathbf{p}) - E(|\mathbf{p} + \mathbf{q}|)], \quad (20)$$

to obtain

$$W_A^{\mu\nu} = \int d^3p dE P(\mathbf{p}, E) \frac{m^2}{E(\mathbf{p})\mathbf{E}(|\mathbf{p} + \mathbf{q}|)} \\ \times [Zw_p^{\mu\nu} + (A - Z)w_n^{\mu\nu}], \quad (21)$$

$A$  and  $Z$  being the target mass number and charge, respectively.

Note that  $w_{p(n)}^{\mu\nu}$  can be directly related to the tensor describing electron scattering off a *free* proton (neutron), carrying momentum  $\mathbf{p}$ , at four momentum transfer  $\tilde{q} \equiv (\tilde{\omega}, \mathbf{q})$ . The effect of nuclear binding is taken into account through the replacement

$$q \equiv (\omega, \mathbf{q}) \rightarrow \tilde{q} \equiv (\tilde{\omega}, \mathbf{q}), \quad (22)$$

reflecting the fact that a fraction  $\delta\omega$  of the energy transfer goes into excitation energy of the spectator system. Therefore, the elementary scattering process is described as if it took place in free space, but with energy transfer  $\tilde{\omega} = \omega - \delta\omega$ .

Within the IA, the non relativistic expression of the longitudinal response reads

$$R_L = \int dE d\mathbf{p} P(\mathbf{p}, E) \left[ \frac{ZG_E^p(\tilde{Q}^2) + (A - Z)G_E^n(\tilde{Q}^2)}{1 + \tilde{Q}^2/(4m^2)} \right] \\ \times \delta[\omega + M_A - E_R - E(|\mathbf{p} + \mathbf{q}|)] \theta(|\mathbf{p} + \mathbf{q}| - k_F) \quad (23)$$

where  $E(|\mathbf{p} + \mathbf{q}|) = m + |\mathbf{p} + \mathbf{q}|^2/(2m)$  and  $E_R = M_R + \mathbf{p}^2/(2M_R)$  are the energies of the knocked out nucleon and the recoiling system, whose mass is given by  $M_R = M_A - m + E$ , respectively.

Note that in the spectral function the state describing the initial nucleon in the interaction vertex is completely antisymmetrized with respect to the other particles in the target nucleus. On the other hand, in the final state only the antisymmetrization of the spectator system is present, while according to the factorization scheme the antisymmetrization of the struck nucleon with respect to the spectator particles is disregarded. As a consequence, the nuclear initial and final states are not orthogonal to one another. In Eq. (23) Pauli's principle is accounted for by requiring the momentum of the knocked out nucleon to be larger than the nuclear Fermi momentum  $k_F = 211$  MeV, determined following the procedure described in Ref. [20]. While this prescription is admittedly rather crude, being based on the local Fermi gas model of the nuclear ground state, it has to be kept in mind that the effect of Pauli blocking rapidly decreases with increasing momentum transfer, and vanishes altogether at  $|\mathbf{q}| \gtrsim 2k_F$ .

Using Eq. (14), we obtain the transverse response

$$R_T = \int dE d\mathbf{p} P(\mathbf{p}, E) [Zr_T^p + (A - Z)r_T^n] \\ \times \delta[\omega + M_A - E_R - E(\mathbf{p} + \mathbf{q})] \theta(|\mathbf{p} + \mathbf{q} - \mathbf{k}_F|), \quad (24)$$

where

$$r_T^p = \left[ -G_E^p{}^2(Q^2) \frac{\mathbf{p}_T^2}{m^2} + \frac{G_M^p{}^2(Q^2)\mathbf{q}^2}{2m^2} \right], \\ r_T^n = \left[ -G_E^n{}^2(Q^2) \frac{\mathbf{p}_T^2}{m^2} + \frac{G_M^n{}^2(Q^2)\mathbf{q}^2}{2m^2} \right]. \quad (25)$$

The relativistic form of the nuclear responses is written in terms of the one-body current

$$j_i^\mu = \frac{(\epsilon_i + \tau\mu_i)}{(1 + \tau)}\gamma^\mu + \frac{(\mu_i - \epsilon_i)}{(1 + \tau)}\frac{i\sigma^{\mu\nu}q_\nu}{2m} \quad (26)$$

where  $\tau = \tilde{Q}^2/(4m^2)$  and  $\epsilon_i$ ,  $\mu_i$  are defined in Eq.(15). In this case, the argument of the energy-conserving  $\delta$ -function, determining the integration limits of the phase-space integration, has to be written using the relativistic expression of the kinetic energies of both the knocked out nucleon and the recoiling spectator system, *i.e.* setting  $E(|\mathbf{p} + \mathbf{q}|) = \sqrt{|\mathbf{p} + \mathbf{q}|^2 + m^2}$  and  $E_R = \sqrt{|\mathbf{p}|^2 + M_R^2}$ .

The GFMC and SF approaches consistently account for NN correlations both in the nuclear ground state and among the (A-1) spectator particles. The continuum contribution to the SF is in fact obtained from the same hamiltonian employed in the GFMC's imaginary time evolution. The main assumption implied in the factorization *ansatz* underlying the IA is that FSI between the struck particle and the spectator system, as well as orthogonality between the initial and final nuclear states, can be neglected in the limit of high momentum transfer. Because the nuclear response is only sensitive to FSI taking place within a distance  $\sim 1/|\mathbf{q}|$  of the electromagnetic vertex, at high momentum transfer this assumption appears to be largely justified. However, FSI effects can be sizable at low momentum transfer, and their effect must be consistently taken into account [19]. In this work, we have followed the scheme developed by the authors of Ref. [20], which proved very effective in describing FSI in electron-carbon scattering in a broad kinematical range.

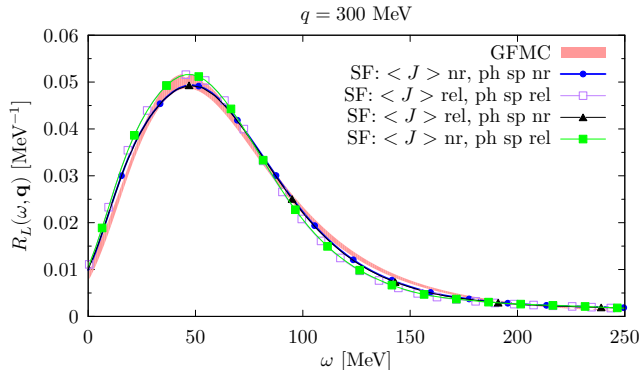


FIG. 1. Electromagnetic response of Carbon in the longitudinal channel at  $|\mathbf{q}| = 300$  MeV. The shaded area shows the results of the GFMC calculation, with the associated uncertainty arising from the inversion of the Euclidean response. All the remaining curves have been obtained within the SF approach, including the effects of Pauli blocking and FSI. The lines marked with dots and hollow squares correspond to non relativistic and fully relativistic calculation, respectively. Those marked with triangles and filled squares have been obtained performing hybrid calculations: non relativistic current and relativistic phase space (triangles), or relativistic current and non relativistic phase space (filled squares).

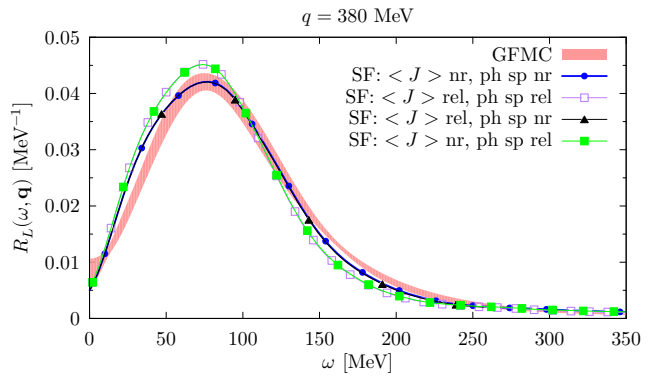


FIG. 2. Same as Fig. 1 for  $|\mathbf{q}| = 380$  MeV.

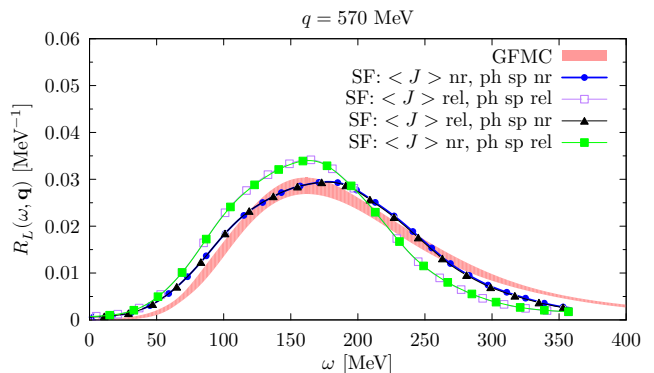


FIG. 3. Same as Fig. 1 for  $|\mathbf{q}| = 570$  MeV.

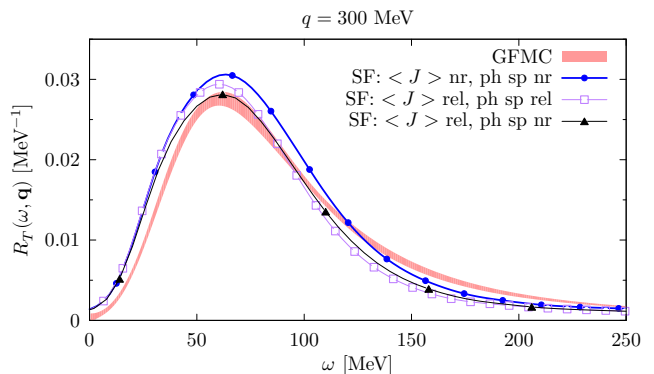


FIG. 4. Electromagnetic response of Carbon in the transverse channel at  $|\mathbf{q}| = 300$  MeV. The shaded area shows the results of the GFMC calculation, with the associated uncertainty arising from the inversion of the Euclidean response. All the remaining curves have been obtained within the SF approach, including the effects of Pauli blocking and FSI. The lines marked with dots and hollow squares correspond to non relativistic and fully relativistic calculation, respectively, while the one marked with triangles has been obtained performing an hybrid calculation: relativistic current and non relativistic phase space.

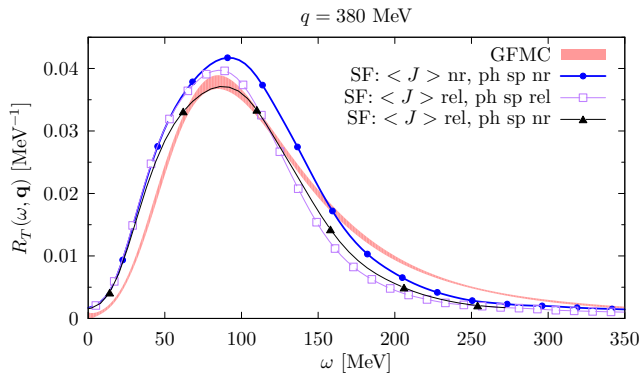


FIG. 5. Same as Fig. 4 for  $|\mathbf{q}| = 380$  MeV.

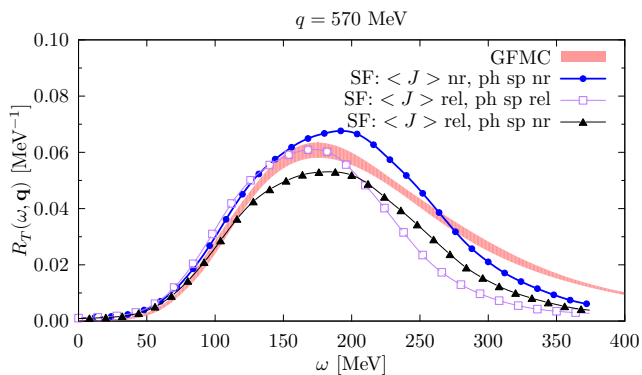


FIG. 6. Same as Fig. 4 for  $|\mathbf{q}| = 570$  MeV.

### III. RESULTS

In Figs. 1, 2, and 3 we show the results of the GFMC and SF calculations of the electromagnetic responses of Carbon in the longitudinal channel, for momentum transfer  $|\mathbf{q}| = 300, 380$  and  $570$  MeV.

Overall, the emerging pattern suggests that—once Pauli blocking and FSI are accounted for—the agreement between the two methods is quite good, provided the non relativistic expression for the current operators and the phase space are consistently employed.

The four different curves labelled SF correspond to the different prescriptions to include relativistic effects. The lines marked with dots and hollow squares represent the non relativistic and fully relativistic results, respectively, while those marked with triangles and filled squares have been obtained performing hybrid calculations, in which the non relativistic expressions have been only used either for the current or for the phase space.

It is apparent that at  $|\mathbf{q}| = 300$  and  $380$  MeV relativistic effects are small. There is little spread between the four SF curves, which are all very close to that corresponding to the GFMC calculation.

At  $|\mathbf{q}| = 570$  MeV, SF and GFMC still give very similar results provided the SF calculation is carried out us-

ing relativistic currents and non relativistic phase space. On the other hand, the results of the fully relativistic calculation and those obtained using non relativistic currents and relativistic phase space clearly show that in this kinematical setup relativistic effects—comprised in the energy conserving  $\delta$ -function—are sizable, and lead to a shift and an enhancement of the peak, whose width is reduced.

In Figs. 4, 5, and 6 we show the electromagnetic response of Carbon in the transverse channel for the same three values of  $|\mathbf{q}|$ .

The agreement between the GFMC and the SF results is not as good as in the longitudinal case. Furthermore, the different behaviour of the curves corresponding to the three SF calculations deserves some comments. As already pointed out in the discussion of the longitudinal responses, a comparison between the relativistic and the hybrid calculations performed with the non relativistic phase space clearly shows that using relativistic kinetic energies in the argument of the energy-conserving  $\delta$ -function results in a shift and an enhancement of the peak of the response. However, unlike the longitudinal one, the transverse response is strongly affected by relativistic effects arising from the treatment of the current operator. This feature clearly manifests itself in the different shapes exhibited by the results of the non relativistic SF calculations and those of the hybrid calculations performed using relativistic currents and non relativistic kinetic energies.

### IV. CONCLUSIONS

The electromagnetic response functions of carbon in the longitudinal and transverse channels have been evaluated within the GFMC and SF approaches at momentum transfer  $|\mathbf{q}| = 300, 380$  and  $570$  MeV.

Because all calculations have been carried out using the same nuclear Hamiltonian and current operator, the resulting response functions can be meaningfully compared, to shed light on the limits of applicability of both the IA, providing the basis of the SF formalism, and the non relativistic approximation inherent in the GFMC method.

Overall, we find that the GFMC results are in remarkably good agreement with those obtained from the SF approach using non relativistic kinetic energies and currents, provided corrections arising from FSI and Pauli blocking are taken into account.

The emerging pattern strongly suggests that the factorization approximation can be safely used down to momentum transfer as low as  $\sim 300$  MeV. This is the first important finding of our study.

In the longitudinal channel relativistic effects are quite small at momentum transfer  $300$  and  $380$  MeV. At  $|\mathbf{q}| = 570$  MeV they become sizable, and arise mainly from the use of relativistic kinetic energies in the argument of the energy-conserving  $\delta$ -function. The significant

reduction of the width can be easily understood considering that its value, while increasing linearly with  $|\mathbf{q}|$  in the non relativistic case, becomes constant and independent of momentum transfer in the relativistic regime.

The interpretation of the results in the transverse channel is more complex. Within the factorization scheme, the main elements entering the definition of the nuclear response are the nuclear amplitudes and the matrix elements of the nuclear current operators. Hence, the accuracy of the results obtained from this approach depends on the treatment of these two quantities. In particular, the degree of complexity of the interaction vertex determines the level of accuracy required in the calculation of the nuclear spectral function.

As an example, consider that in the transverse channel the matrix element of the current contains terms linear in the momentum of the struck particle. However, since the spectral function of Ref. [32], employed to carry out our calculations, is spherically symmetric, they do not contribute to the responses. A more accurate treatment of the carbon ground state, taking into account its deformation, would allow to include the contributions arising from these terms.

Contrary to what is observed in the longitudinal channel, in the transverse responses, relativistic effects are to be ascribed not only to the arguments of the energy-conserving  $\delta$ -function, but also to the treatment of the current operator. The fact that for large values of the momentum transfer relativistic corrections to the trans-

verse one-body current are important suggests that improving the non relativistic expansion with the inclusion of terms  $\mathcal{O}[(|\mathbf{q}|/m)^2]$  may be needed obtain a more accurate prediction of the response.

The analysis reported in this paper provides valuable and novel information, much needed to reach a better understanding of the description of the nuclear cross section obtained from different *ab initio* approaches. Our study obviously needs to be completed including the contributions of two-nucleon currents, which are known to be important in the transverse channel. Work towards the achievement of this goal is underway.

## ACKNOWLEDGMENTS

Many illuminating discussions and a critical reading of the manuscript by Rocco Schiavilla are gratefully acknowledged. NR thanks the Theory Group at TRIUMF for its hospitality and for partial support during the completion of this work. The work of NR has been partially supported by the Spanish Ministerio de Economía y Competitividad and European FEDER funds under the contracts FIS2014-51948-C2-1-P. The work of OB and NR was supported by INFN under grant MANYBODY. The work of AL was supported by the U.S. Department of Energy, Office of Science, Office of Nuclear Physics, under contract DE-AC02-06CH11357.

- 
- [1] R. Acciarri *et al.* (ArgoNeuT), Phys. Rev. D **90**, 012008 (2014).
- [2] F. Cavanna, O. Palamara, R. Schiavilla, M. Soderberg, and R. B. Wiringa, (2015), arXiv:1501.01983 [nucl-ex].
- [3] A. A. Aguilar-Arevalo *et al.* (MiniBooNE), Phys. Rev. Lett. **100**, 032301 (2008), arXiv:0706.0926 [hep-ex].
- [4] A. A. Aguilar-Arevalo *et al.* (MiniBooNE), Phys. Rev. **D81**, 092005 (2010), arXiv:1002.2680 [hep-ex].
- [5] M. Martini, M. Ericson, G. Chanfray, and J. Marteau, Phys. Rev. **C80**, 065501 (2009), arXiv:0910.2622 [nucl-th].
- [6] M. Martini, M. Ericson, G. Chanfray, and J. Marteau, Phys. Rev. **C81**, 045502 (2010), arXiv:1002.4538 [hep-ph].
- [7] J. Nieves, I. Ruiz Simo, and M. J. Vicente Vacas, Phys. Rev. **C83**, 045501 (2011), arXiv:1102.2777 [hep-ph].
- [8] J. Nieves, I. Ruiz Simo, and M. J. Vicente Vacas, Phys. Lett. **B707**, 72 (2012), arXiv:1106.5374 [hep-ph].
- [9] J. E. Amaro, M. B. Barbaro, J. A. Caballero, T. W. Donnelly, and C. F. Williamson, Phys. Lett. **B696**, 151 (2011), arXiv:1010.1708 [nucl-th].
- [10] G. D. Megias *et al.*, Phys. Rev. **D91**, 073004 (2015), arXiv:1412.1822 [nucl-th].
- [11] G. D. Megias *et al.*, arXiv:1607.08565 [nucl-th].
- [12] S. Bacca, N. Barnea, G. Hagen, G. Orlandini, and T. Papenbrock, Phys. Rev. Lett. **111**, 122502 (2013), arXiv:1303.7446 [nucl-th].
- [13] S. Bacca, N. Barnea, G. Hagen, M. Miorelli, G. Orlandini, and T. Papenbrock, Phys. Rev. **C90**, 064619 (2014), arXiv:1410.2258 [nucl-th].
- [14] A. Lovato, S. Gandolfi, J. Carlson, S. C. Pieper, and R. Schiavilla, Phys. Rev. **C91**, 062501 (2015), arXiv:1501.01981 [nucl-th].
- [15] A. Lovato, S. Gandolfi, J. Carlson, S. C. Pieper, and R. Schiavilla, Phys. Rev. Lett. **117**, 082501 (2016), arXiv:1605.00248 [nucl-th].
- [16] O. Benhar, N. Farina, H. Nakamura, M. Sakuda, and R. Seki, Phys. Rev. D **72**, 053005 (2005).
- [17] O. Benhar, A. Lovato, and N. Rocco, Phys. Rev. C **92**, 024602 (2015), arXiv:1502.00887 [nucl-th].
- [18] N. Rocco, A. Lovato, and O. Benhar, Phys. Rev. Lett. **116**, 192501 (2016), arXiv:1512.07426 [nucl-th].
- [19] O. Benhar, Phys. Rev. C **87**, 024606 (2013).
- [20] A. M. Ankowski, O. Benhar, and M. Sakuda, Phys. Rev. D **91**, 054616 (2015).
- [21] R. B. Wiringa, V. G. J. Stoks, and R. Schiavilla, Phys. Rev. **C51**, 38 (1995), arXiv:nucl-th/9408016 [nucl-th].
- [22] S. C. Pieper, V. R. Pandharipande, R. B. Wiringa, and J. Carlson, Phys. Rev. **C64**, 014001 (2001), arXiv:nucl-th/0102004 [nucl-th].
- [23] L. E. Marcucci, F. Gross, M. T. Pena, M. Piarulli, R. Schiavilla, I. Sick, A. Stadler, J. W. Van Orden, and M. Viviani, J. Phys. **G43**, 023002 (2016), arXiv:1504.05063 [nucl-th].
- [24] J. J. Kelly, Phys. Rev. C **70**, 068202 (2004).
- [25] R. Bradford, A. Bodek, H. Budd, and J. Arrington, Nucl.



- Phys. B Proc. Suppl. **159**, 127 (2006).
- [26] J. Carlson, S. Gandolfi, F. Pederiva, S. C. Pieper, R. Schiavilla, K. E. Schmidt, and R. B. Wiringa, Rev. Mod. Phys. **87**, 1067 (2015), arXiv:1412.3081 [nucl-th].
- [27] J. Carlson and R. Schiavilla, Phys. Rev. Lett. **68**, 3682 (1992).
- [28] J. Carlson and R. Schiavilla, Phys. Rev. **C49**, R2880 (1994).
- [29] J. Carlson, J. Jourdan, R. Schiavilla, and I. Sick, Phys. Rev. **C65**, 024002 (2002), arXiv:nucl-th/0106047 [nucl-th].
- [30] R. Bryan, European Biophysics Journal **18**, 165 (1990).
- [31] M. Jarrell and J. E. Gubernatis, Phys. Rept. **269**, 133 (1996).
- [32] O. Benhar, A. Fabrocini, S. Fantoni, and I. Sick, Nucl. Phys. A **579**, 493 (1994).